

# Experimental demonstration of entanglement distillation under LOCC operations

Zhi-Wei Wang,\* Xiang-Fa Zhou,<sup>†</sup> Yun-Feng Huang, Yong-Sheng Zhang, Xi-Feng Ren, and Guang-Can Guo<sup>‡</sup>

*Key Laboratory of Quantum Information, University of Science and Technology of China, CAS, Hefei 230026, People's Republic of China*

We experimentally demonstrate optimal entanglement distillation from two forms of two-qubit mixed states under local filtering operations according to the constructive method introduced by F. Verstraete *et al.* [Phys. Rev. A 64, 010101(R) (2001)]. In principle, our set-up can be easily applied to distilling entanglement from arbitrary two-qubit partially mixed states. We also test the violation of the Clauser-Horne-Shimony-Holt(CHSH) inequality for the distilled state from the first form of mixed state to show its "hidden non-locality".

PACS number(s): 03.67.Mn, 03.65.Ud, 42.50.Dv, 42.65.Lm

## I. INTRODUCTION

Entanglement plays a key role in quantum information processing, such as quantum teleportation [1], efficient quantum computation [2] and entangled-assisted quantum cryptography [3]. In general, these applications require maximally entangled quantum states. However, owing to decoherence and dissipation, practical states are normally less entangled or partially mixed. To cope with this problem, entanglement concentration is essential [4] and various schemes have been proposed [5, 6, 7, 8]. Experimentally Kwiat *et al.* implemented entanglement distillation from non-maximally entangled pure state and one special kind of two-qubit mixed state using partial polarizers [9]. After that, entanglement concentration from maximally entangled mixed states (MEMS) has also been realized using similar method [10].

Generally speaking, there are two types of concentration protocols: those involving collective operations performed on many copies of the state and those working on individual copies. The latter case is of special interest in practical protocols, because usually there might be technologic difficulties to implement collective operations. For this case, although some experiments on certain kind of two-qubit mixed states have been experimentally demonstrated [9, 10], it is still interesting to explore what is the best we can do to distill entanglement from arbitrary two-qubit mixed states, only allowing local operations and classical communication (LOCC) to be performed on each copy separately. In [7], Kent *et al.* proved that the best state one can obtain from general two-qubit mixed states is a Bell diagonal state. After that, F. Verstraete *et al.* constructively gave out the optimal local filtering operations for distilling entanglement from an arbitrary two-qubit mixed state [11]. In this paper, we experimentally demonstrate optimal entanglement distillation from two forms of two-qubit mixed states which frequently exist in the real world. The optimal local filtering operations are explicitly calculated according to the method provided in [11]. And in principle, our set-up can be applied to entanglement distillation of arbitrary two-qubit mixed states.

For general two-qubit mixed states, consider two separated parts, Alice and Bob, who each control one subsystem and are only allowed to carry out local operations and classical communications. Specifically, Alice and Bob are only permitted to perform local unitary transformations and local filterings. Then what we are concerned about is whether they can increase the entanglement of the system and to what extent they can do that under LOCC. This problem is very interesting because any real world quantum communication channel is imperfect and generally, Alice and Bob are not able to share perfect maximally entangled states directly.

Theoretically, by introducing the real and linear parametrization, a two-qubit density matrix can be represented as

$$\rho = \frac{1}{4} \sum_{i,j=0}^3 R_{ij} \sigma_i \otimes \sigma_j, \quad (1)$$

where  $\sigma_0$  is the  $2 \times 2$  identity and  $\sigma_1, \sigma_2, \sigma_3$  are usual Pauli matrices. LOCC of the type  $\rho' \sim (A \otimes B)\rho(A \otimes B)^\dagger$  corresponds to left and right multiplication by a proper orthochronous Lorentz transformation (POLT), followed

---

\*Electronic address: sdzzwzw@mail.ustc.edu.cn

<sup>†</sup>Electronic address: xfzhou@mail.ustc.edu.cn

<sup>‡</sup>Electronic address: gcguo@ustc.edu.cn

by normalization in this  $R$ -picture. Optimal concentration operations have been obtained in [11] for two cases. If  $R = [R_{ij}]$  is diagonalizable by PLOT, a Bell diagonal mixed state can be extracted from the input state with a finite probability, which has the maximal entanglement of formation (EoF) [7] and the maximal possible violation of the Clauser-Horne-Shimony-Holt (CHSH) version of inequality [12, 13]. When  $R$  is not diagonalizable by PLOT, the initial state can be quasi-distillable. In the extreme case, the input state can be asymptotically transformed into a Bell diagonal state with lower rank, while the success probability becomes infinitesimally close to zero.

## II. THE EXPERIMENTS FOR ENTANGLEMENT DISTILLATION AND THE TEST OF CHSH INEQUALITY

Experimentally, to demonstrate the optimal entanglement distillation protocol, we concentrate on the mixed states that can be diagonalized by PLOT. We specially devise two forms of two-qubit mixed states which can be easily prepared and concentrated under fewer local operations. The experiment set-up to investigate entanglement distillation is shown in Fig. 1. A 0.59 mm thick  $\beta$ -barium borate (BBO) crystal arranged in the Kwiat type configuration [14] is pumped by a 351.1 nm laser beam produced by an  $\text{Ar}^+$  laser. In the spontaneous parametric down-conversion (SPDC) process, a nonmaximally entangled state  $a|HH\rangle + b|VV\rangle$  ( $H$  and  $V$  represent horizontal and vertical polarization of the photons respectively) is produced, where the real numbers  $a$  and  $b$  can be determined by the polarization of the pump beam and the normalization condition  $a^2 + b^2 = 1$ . After the BBO crystal, the photon pairs pass through two phase-damping channels in a particular basis. In our scheme, each phase-damping channel consists of one quartz plate with its optical axis rotated by a certain angular to the vertical axis. For the first form of mixed state, we select two same phase-damping channels in  $\{H + V, H - V\}$  basis with the corresponding super-operators  $\{\sqrt{1-p}I, \sqrt{p}\sigma_x\}_A \otimes \{\sqrt{1-p}I, \sqrt{p}\sigma_x\}_B$ , where  $p$  is connected with the thickness of the quartz and the bandwidth of the interference filter [15]. Then the mixed state has the form

$$\rho_I = \begin{pmatrix} (p-1)^2 + b^2(2p-1) & 0 & 0 & ab((p-1)^2 + p^2) \\ 0 & p-p^2 & 2abp(1-p) & 0 \\ 0 & 2abp(1-p) & p-p^2 & 0 \\ ab((p-1)^2 + p^2) & 0 & 0 & p^2 - b^2(2p-1) \end{pmatrix}, \quad (2)$$

In the experiment, we choose  $a = 0.23$ ,  $b = 0.97$ , and  $p = 0.013$  ( $a \sim 1.5$ -mm-thick quartz plate).

According to Ref. [11], the local operations for Alice and Bob are  $\begin{pmatrix} 1 & 0 \\ 0 & 0.49 \end{pmatrix}$  and  $\begin{pmatrix} 0 & 1 \\ 1 & 0 \end{pmatrix} \begin{pmatrix} 1 & 0 \\ 0 & 0.49 \end{pmatrix}$  respectively.

For Alice, the filtering operation can be realized by inserting into her path microscope slides tilted about the vertical axis  $73^\circ$ . This configuration has a measured transmission of 92% for  $H$  polarization and 22% for  $V$  polarization. As for Bob, there are a local filtering and a single-qubit unitary operation. He just needs to place a half wave plate (HWP) after the microscope slides with the angle between the optical axis and the vertical axis set to  $45^\circ$ . We can also realize the local filtering operation using a Mach-Zehnder interferometer [16], but it requires too much about its stability and visibility.

To obtain the density matrices of the distilled states, we use the technology of maximum likelihood tomography [14, 17]. By means of a quarter wave plate (QWP), HWP and polarizing beam splitter (PBS) in each arm, the polarization of each photon can be analyzed in an arbitrary basis. Then by combinations of 16 single-photon projections  $|H\rangle$ ,  $|V\rangle$ ,  $|H\rangle + |V\rangle$ ,  $|H\rangle + i|V\rangle$  on each of the two-photon, we may derive the density matrices describing the states of the photon pairs. Fig. 2 shows the density matrices before and after entanglement distillation.

Here we use concurrence [18] to characterize the entanglement between the two subsystems. The concurrence before and after distillation are  $0.248 \pm 0.021$  and  $0.672 \pm 0.044$  respectively. The distilled state  $\rho_2$  (all the experimental density matrices can be found in APPENDIX) has the fidelity of [19] 82% with the theoretical Bell diagonal state. From the data we can see that by means of the local filtering operations we can effectively increase the entanglement between the two subsystems. The errors mainly stem from the imperfect preparation of the initial mixed state  $\rho_1$  (the fidelity is 94%) and in the case of strong filtering, small changes in the initial state will have a large impact on the final state.

We also find the “hidden non-locality” of the distilled state by its violation CHSH version of inequality. In the CHSH inequality, the proposed value  $|S|$ , a combination of four polarization correlation probabilities, should not be more than 2 for local hidden variables (LHV) theory. If  $|S| > 2$ , we can only use quantum mechanics to explain the correlations. Experimentally, the set-up for tomographic reconstruction can also be used for the measurement of the CHSH inequality. The analysis settings of QWPs and HWPs are determined by the tomographically measured density matrix of each state using the method introduced in Ref. [20]. Following the normalization procedure [21], we obtain the value  $S_{\text{before}} = 1.853 \pm 0.011$  and  $S_{\text{after}} = 2.175 \pm 0.024$ , corresponding to the values of  $S$  before and after the entanglement distillation. Thus we obtain the violation of about  $7\sigma$ . In the process of entanglement

distillation, Alice and Bob only employ LOCC operations. As pointed by Kwiat [9], the non-locality demonstrations rely on “conditional probabilities”: we use LOCC operations to select a subensemble with a small probability which can demonstrate non-local correlations. This idea is similar to entanglement distillation: we can just increase the entanglement of subensemble and can not do that for the whole ensemble [22].

Next consider distilling the entanglement from the other form of two-qubit mixed state. This time we let the nonmaximally entangled states pass through two same phase-damping channels in  $\{H, V\}$  basis. The corresponding super-operators are  $\{\sqrt{1-p}I, \sqrt{p}\sigma_z\}_A \otimes \{\sqrt{1-p}I, \sqrt{p}\sigma_z\}_B$ . Each channel is a  $\sim 3$  mm quartz which has a polarization-dependent optical path length difference about  $40\lambda$  ( $\lambda = 702.2$  nm). After the decoherence, the state has the form

$$\rho_{II} = \begin{pmatrix} a^2 & 0 & 0 & ab(-1+2p)^2 \\ 0 & 0 & 0 & 0 \\ 0 & 0 & 0 & 0 \\ ab(-1+2p)^2 & 0 & 0 & b^2 \end{pmatrix}. \quad (3)$$

For this kind of mixed states, the only local operation is just a unilateral local filtering  $\begin{pmatrix} b & 0 \\ 0 & a \end{pmatrix}$  for Bob. We consider two cases ( $a = 0.44, 0.52$  and  $p = 0.063$ ). The experiment results are shown in Fig. 3. Under this local filtering operation, the entanglement of the final states can be increased. For  $a = 0.44$ , the concurrence increases from  $0.552 \pm 0.017$  (for  $\rho_3$ ) to  $0.641 \pm 0.022$  (for  $\rho_4$ ); the fidelities with the corresponding theoretical states are 98% and 96% respectively. For  $a = 0.52$ , the concurrence increases from  $0.569 \pm 0.017$  (for  $\rho_5$ ) to  $0.666 \pm 0.021$  (for  $\rho_6$ ); the fidelities with the corresponding theoretical states are 97% and 97% respectively.

### III. DISCUSSION AND CONCLUSION

In this paper, we have experimentally demonstrated optimal local filtering operations for two general forms of two-qubit mixed states that can be diagonalized by POLT. For the first form of mixed state, the local operations involve bilateral filtering; while for the second one, only unilateral filtering is needed. In fact, we can generalize this method to arbitrary two-qubit partially mixed states, because any nontrivial LOCC operations have the form [7, 16]

$$\gamma U_A \begin{pmatrix} 1 & 0 \\ 0 & \alpha_A \end{pmatrix} U'_A \otimes U_B \begin{pmatrix} 1 & 0 \\ 0 & \alpha_B \end{pmatrix} U'_B, \quad (4)$$

where  $U_{A(B)}$  and  $U'_{A(B)}$  denote local unitary operations for Alice (Bob) and  $\gamma$  is a scale factor in the range  $0 \leq \gamma \leq 1$  and  $0 \leq \alpha_{A(B)} \leq 1$ . The main experiment difficulty lies in the preparation of arbitrary two-qubit mixed states.

On the other hand, the imperfect preparation of initial mixed states is also a main reason for the deviations of our results from theoretical calculation. However, in practical schemes, one can directly choose the states derived from the tomographic measurement of the input as the initial mixed states and implement corresponding local filtering operations on them. Thus the experiment results will approach the theory with better accuracy. After the local filtering operations, Bell diagonal states can be obtained from the input states which have the maximum concurrence and the maximum possible violation of the CHSH inequality. We experimentally obtain the violation of the CHSH inequality about  $7\sigma$  for the distilled state from the first form of mixed state, which verifies “hidden non-locality” for this form of mixed state in the process of entanglement distillation. Recently it has been found that Bell diagonal states can also be used to implement the generalized tomographic quantum key distribution protocol [23]. The method used in this experiment is very simple and universal since it just needs LOCC operations and it can effectively increase the entanglement of arbitrary two-qubit partially mixed states. We believe it will be helpful in the exploration of various quantum information processing.

### ACKNOWLEDGMENTS

The authors would like to thank Fang-Wen Sun and Guo-Yong Xiang for helpful discussions. This work was funded by the National Fundamental Research Program (2001CB309300), National Natural Science Foundation of China (10304017, 10404027), the Innovation Funds from Chinese Academy of Sciences.

### APPENDIX

The explicit density matrices of  $\rho_i (i = 1, 2, \dots, 6)$  are listed below:

$$\rho_1 = \begin{pmatrix} 0.0435 & 0.0260 + i0.0215 & 0.0197 - i0.0126 & 0.1273 + i0.0592 \\ 0.0260 - i0.0215 & 0.0320 & 0.0053 - i0.0208 & 0.0867 - i0.0746 \\ 0.0197 + i0.0126 & 0.0053 + i0.0208 & 0.0295 & 0.0711 + i0.0614 \\ 0.1273 - i0.0592 & 0.0867 + i0.0746 & 0.0711 - i0.0614 & 0.8949 \end{pmatrix}, \quad (a)$$

$$\rho_2 = \begin{pmatrix} 0.0831 & 0.1594 - i0.0459 & 0.1393 - i0.0418 & -0.0288 - i0.0207 \\ 0.1594 + i0.0459 & 0.3665 & 0.3388 + i0.0686 & -0.0160 - i0.0530 \\ 0.1393 + i0.0418 & 0.3388 - i0.0686 & 0.4854 & 0.0005 - i0.0804 \\ -0.0288 + i0.0207 & -0.0160 + i0.0530 & 0.0005 + i0.0804 & 0.0649 \end{pmatrix}, \quad (b)$$

$$\rho_3 = \begin{pmatrix} 0.2062 & 0.0509 + i0.0054 & 0.0091 - i0.0116 & 0.2754 + i0.0247 \\ 0.0509 - i0.0054 & 0.0135 & 0.0013 - i0.0047 & 0.0531 - i0.0106 \\ 0.0091 + i0.0116 & 0.0013 + i0.0047 & 0.0048 & 0.0421 - i0.0064 \\ 0.2754 - i0.0247 & 0.0531 + i0.0106 & 0.0421 + i0.0064 & 0.7754 \end{pmatrix}, \quad (c)$$

$$\rho_4 = \begin{pmatrix} 0.5204 & 0.1112 + i0.0122 & 0.0029 - i0.0005 & 0.3139 + i0.0652 \\ 0.1112 - i0.0122 & 0.0250 & -0.0008 & 0.0539 + i0.0027 \\ 0.0029 + i0.0005 & -0.0008 & 0.0034 & 0.0178 + i0.0043 \\ 0.3139 - i0.0652 & 0.0539 - i0.0027 & 0.0178 - i0.0043 & 0.4512 \end{pmatrix}, \quad (d)$$

$$\rho_5 = \begin{pmatrix} 0.2697 & 0.0593 + i0.0033 & 0.0104 - i0.0068 & 0.2810 + i0.0511 \\ 0.0593 - i0.0033 & 0.0139 & 0.0012 - i0.0025 & 0.0462 - i0.0003 \\ 0.0104 + i0.0068 & 0.0012 + i0.0025 & 0.0045 & 0.0366 - i0.0011 \\ 0.2810 - i0.0511 & 0.0462 + i0.0003 & 0.0366 + i0.0011 & 0.7119 \end{pmatrix}, \quad (e)$$

$$\rho_6 = \begin{pmatrix} 0.5212 & 0.0939 + i0.0145 & 0.0076 + i0.0020 & 0.3320 + i0.0333 \\ 0.0939 - i0.0145 & 0.0183 & 0.0001 & 0.0461 - i0.0071 \\ 0.0076 - i0.0020 & 0.0001 & 0.0029 & 0.0244 + i0.0010 \\ 0.3320 - i0.0333 & 0.0461 + i0.0071 & 0.0244 - i0.0010 & 0.4577 \end{pmatrix}. \quad (f)$$

---

[1] C. H. Bennett *et al.*, Phys. Rev. Lett. **70**, 1895 (1993).  
[2] C. H. Bennett and D. P. DiVincenzo, Nature (London) **404**, 247 (2000).  
[3] A. K. Ekert, Phys. Rev. Lett. **67**, 661 (1991).  
[4] C. H. Bennett, H. J. Bernstein, S. Popescu, and Schumacher, Phys. Rev. A **53**, 2046 (1996); C. H. Bennett *et al.*, Phys. Rev. Lett. **76**, 722 (1996).  
[5] N. Gisin, Phys. Lett. A **210**, 151 (1996).  
[6] M. Horodecki, P. Horodecki, and R. Horodecki, Phys. Rev. Lett. **78**, 574 (1997).  
[7] A. Kent, N. Linden, and S. Massar, Phys. Rev. Lett. **83**, 2656 (1999).  
[8] R. T. Thew and W. J. Munro, Phys. Rev. A **63** 030302(R) (2001); R. T. Thew and W. J. Munro, Phys. Rev. A **64**, 022320 (2001).  
[9] P. G. Kwiat, S. Barraza-Lopez, A. Stefanov, and N. Gisin, Nature (London) **409**, 1014 (2001).  
[10] N. A. Peters, J. B. Altepeter, D. Branning, E. R. Jeffrey, Tzu-Chieh Wei, and P. G. Kwiat, Phys. Rev. Lett. **92**, 133601 (2004).  
[11] F. Verstraete, J. Dehaene, and B. DeMoor, Phys. Rev. A **64**, 010101(R) (2001).  
[12] F. Verstraete and M. M. Wolf, Phys. Rev. Lett. **89**, 170401 (2002).  
[13] J. Clauser, M. Horne, S. Shimony, and R. Holt, Phys. Rev. Lett. **23**, 880 (1969).  
[14] A. G. White *et al.*, Phys. Rev. Lett. **83**, 3103 (1999).  
[15] A. J. Berglund, e-print quant-ph/0010001; Y.-S. Zhang, Y.-F. Huang, C.-F. Li, and G.-C. Guo, e-print quant-ph/0206166.  
[16] C. Zhang, Quantum Inf. Comput. **4**, 196 (2004).  
[17] D. F. V. James, P. G. Kwiat, W. J. Munro, and A. G. White, Phys. Rev. A **64**, 052312 (2001).  
[18] S. Hill and W. K. Wootters, Phys. Rev. Lett. **78**, 5022 (1997); W. K. Wootters, Phys. Rev. Lett. **80**, 2245 (1998).

[19] Here the fidelity between two states  $\rho_{in}$  and  $\rho_{out}$  is defined as

$$|Tr(\sqrt{\sqrt{\rho_{in}}\rho_{out}\sqrt{\rho_{in}}})|^2.$$

[20] R. Horodecki, P. Horodecki, and M. Horodecki, Phys. Lett. A **200**, 340 (1995).

[21] A. Aspect, P. Grangier, and G. Roger, Phys. Rev. Lett. **49**, 91 (1982).

[22] C. H. Bennett, H. J. Bernstein, S. Popescu, and B. Schumacher, Phys. Rev. A **53**, 2046 (1996).

[23] D. Kaszlikowski, J. Y. Lim, D. K. L. Oi, F. H. Willeboordse, A. Gopinathan, and L. C. Kwek Phys. Rev. A **71**, 012309 (2005).

**FIG. 1** Experimental arrangement to implement entanglement distillation. The half wave plate (HWP), quarter wave plate (QWP) and BBO crystal in the pump beam are used to prepare nonmaximally entangled states. In the mixed state preparation process, we use quartz plates as decoherence channels which can be rotated to introduce decoherence in a particular basis. The local operations are realized using microscope slides and HWPs. To distill entanglement from the first form of mixed state, the local operations involve bilateral filterings. For the second form of mixed state, only unilateral filtering is needed. The final QWP and HWP, together with polarizing beam splitter (PBS) in each arm, enable analysis of the polarization correlations in any basis, which can be applied to tomographic measurement and Bell inequality analysis. To detect the photon pairs, we use interference filters (bandwidth 4.62 nm), single-photon detectors and two-photon coincidence.

**FIG. 2** Experimental data for the first form of mixed state. Density matrices  $\rho_1$  and  $\rho_2$  corresponding to the states before and after the entanglement distillation are shown in Figure (1) and (2). The fidelities with the corresponding theoretical states are 94% and 82%.

**FIG. 3** Experimental data for the second form of mixed state. Density matrices  $\rho_3$  and  $\rho_4$  ( $\rho_5$  and  $\rho_6$ ) are shown in Figure (1)((2)) and (1')((2')) which correspond to the states before and after the entanglement distillation. The fidelities with the corresponding theoretical states are 98%(97%) and 96%(97%).

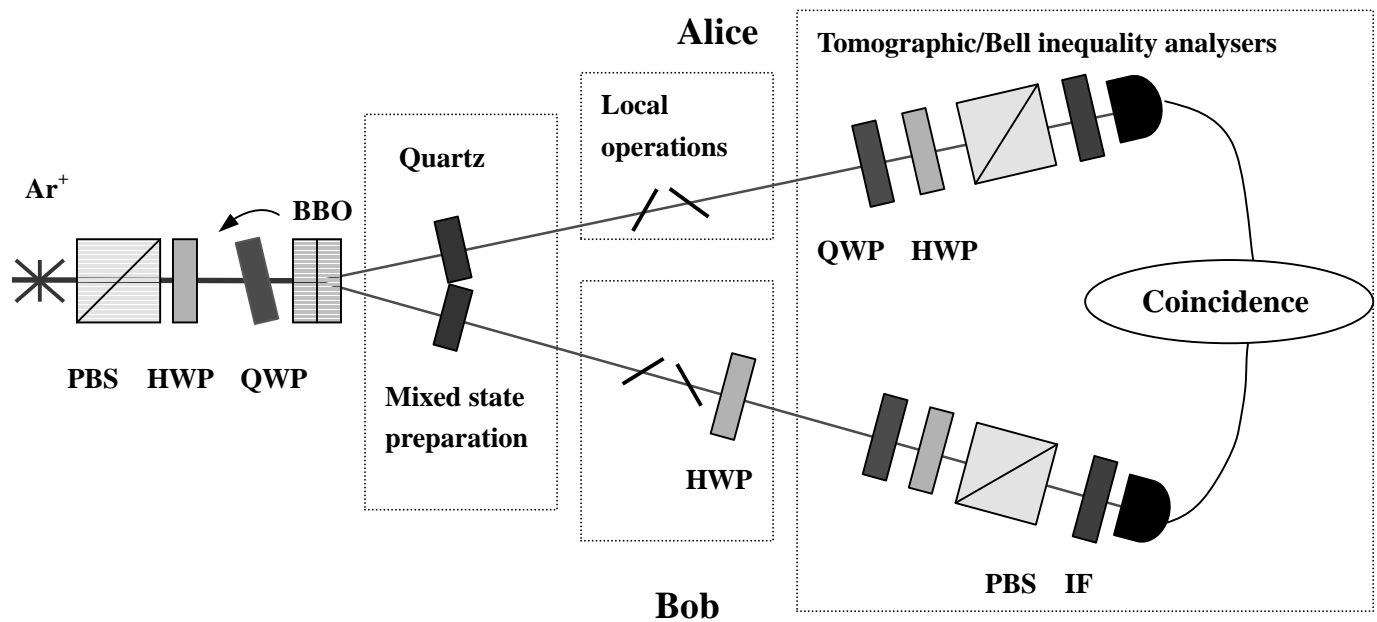
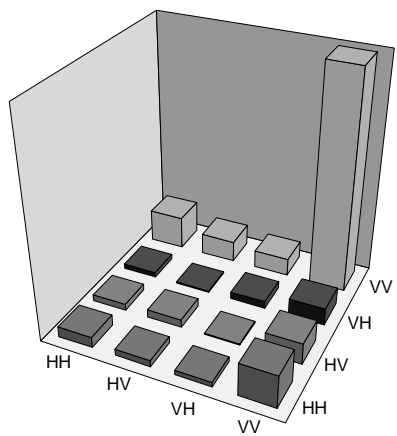


**FIG. 1**

**(1) Before distillation**



**(2) After distillation**

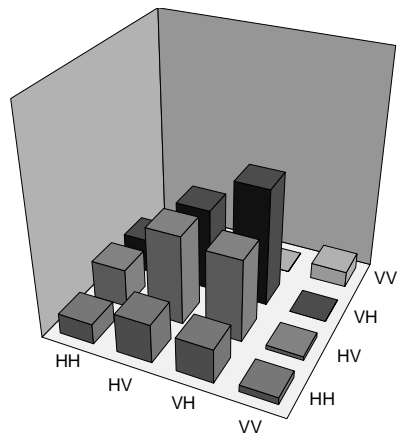
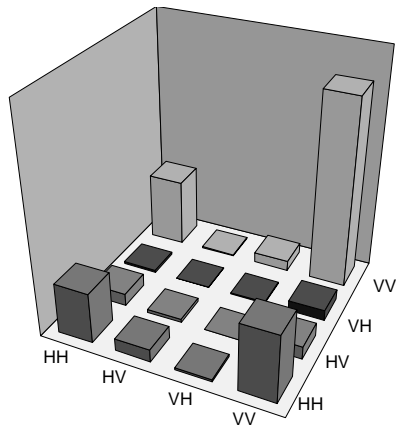
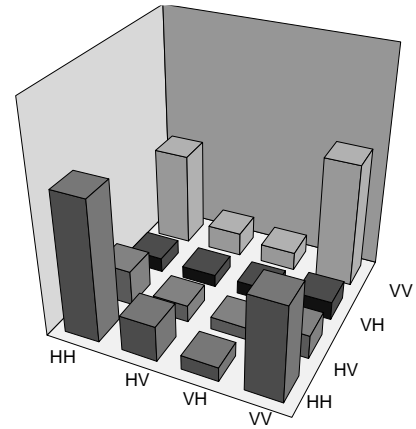


**FIG. 2**

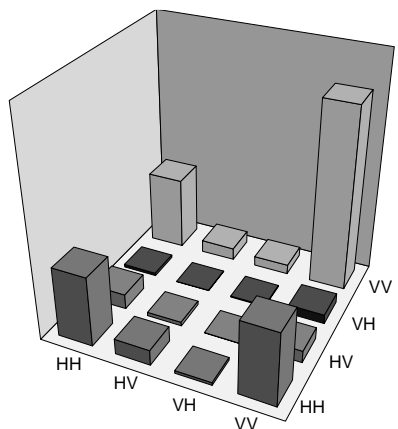
**(1) Before distillation**



**(1') After distillation**



**(2) Before distillation**



**(2') After distillation**

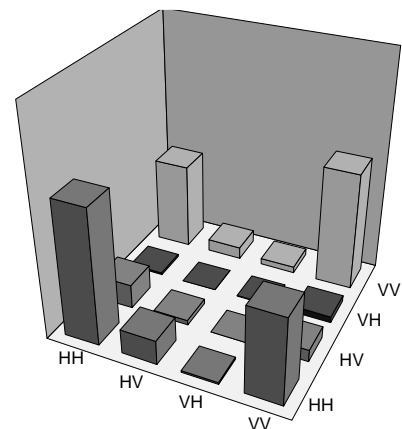


**FIG. 3**